J Supercond Nov Magn (2011) 24: 1273–1280
DOI 10.1007/s10948-010-0822-9

ORIGINAL PAPER

Relevance of the Phonon-Coupling Mode on the Superconducting Pairing Interaction of $La_{2-x}Sr_xCuO_4$

H.S. Ruiz · A. Badía-Majós

Received: 26 May 2010 / Accepted: 12 July 2010 / Published online: 6 August 2010

Abstract Despite the intensive efforts for determining the mechanism that causes high-temperature superconductivity in copper oxide materials (cuprates), no consensus on the pairing mechanism has been reached. Recent advances in angle-resolved photoemission spectroscopies (ARPES) have suggested that a sizeable electron–phonon coupling exists as the principal cause for kinks in the dispersion relations (energy versus wavevector) of the electronic states. Here, we report on a systematic study of the influence of the electron–phonon-coupling parameter "λ" in the electronic quasiparticle dispersions along the nodal direction for $La_{2-x}Sr_xCuO_4$, covering the entire doping range over which the electron transport properties vary from insulating ($0 \lesssim x \lesssim 0.03$) to superconducting ($0.05 \lesssim x \lesssim 0.25$) and eventually non-superconducting metal ($x > 0.25$). This includes our recently introduced theoretical model to adjust the experimental data on the fermionic band dispersion. The coupling constant λ, calculated consistently with the nodal kink dispersions, reproduces the observed critical temperatures T_c, the gap ratio $2\Delta_0/k_BT_c$, and other parameters which have been studied from several equations. Our results suggest that, at least in $La_{2-x}Sr_xCuO_4$, electron–phonon coupling is the most relevant boson-coupling mode to influence the electron dynamics, and must therefore be included in any microscopic theory of superconductivity.

Keywords Kink · Electron–phonon interaction

H.S. Ruiz (✉) · A. Badía-Majós
Departamento de Física de la Materia Condensada – I.C.M.A.,
Universidad de Zaragoza – C.S.I.C., María de Luna 3,
50018 Zaragoza, Spain
e-mail: hsruizr@unizar.es

1 Introduction

For the detailed understanding of the microscopic processes involved in the high-temperature superconducting copper oxides (HTSC), it is important to determine the dynamics of the electronic band structure within the energy-momentum space. This includes the low- and high-energy excitations both for the normal- and superconducting-states, the Fermi surface, and the superconducting gap and pseudogap. Nowadays, such information is available thanks to the advent of improved resolution both in energy and momentum in angle-resolved photoemission spectroscopy (ARPES), inelastic neutron scattering (INS), and x-ray scattering (IXS) experiments [1]. These advances have led to new findings through efficient Fermi surface mapping, fine electronic structure resolving, and direct determination of the electron self-energy. In order to understand the relevance of the ARPES technique, we recall that the photoemission process results in both an excited photoelectron and a photohole in the final state. Related to this observation, it becomes a useful probe of the related scattering mechanisms contributing to the electrical transport in different materials. Unlike other probes of the transport properties, the ARPES technique has the advantage of momentum resolving. Along this line, we want to note that the single-particle scattering rate measured in ARPES is not identical to the scattering rate measured in transport studies. Nonetheless, direct proportionality between them has been established [2, 3].

Noticeably, the ARPES measurements show a small anomaly known as a "kink", which appears as a sudden change in the quasiparticle energy dispersion in the vicinity of Fermi level (E_F) [4]. This feature, so far universal to HTSC [5], has been regarded as a signature of the interaction between electrons with boson excitations (phonons or spin fluctuations), which causes the pairing and leads

to superconductivity. Then, an appropriate theoretical interpretation of the dispersion relations involved is highly desirable as a basis for the study of the superconductor pairing mechanism, the quasiparticle properties (thermodynamic), and the transport properties in HTSC. So far, the origin of high-temperature superconductivity and the nature of the bosons involved remains controversial mainly because experiments can only be used to determine an approximate energy of the mode and this energy is close to both the optical phonons [4, 6–10] and magnetic excitations [11–16]. Related to this, the energy scales of the optical phonons in the CuO_2 planes are similar between electron and hole doped cuprates, while the magnetic mode for electron doped HTSC is found to be much smaller [17, 18]. Along this line, S.R. Park et al. [19] have recently demonstrated that the magnetic resonance mode cannot explain the ARPES spectra in several electron doped HTSC systems showing a clear support for the electron–phonon coupling.

Some additional facts related to the electron–phonon pairing mechanism are to be mentioned. J. Graf et al. [7] have recently reported the first evidence of an anomalous dispersion of the Cu–O bond-stretching phonon mode in a Bi cuprate, supporting the idea that strong electron energy dispersion measured by ARPES corresponds to the Cu–O bond-stretching phonon mode. On the other hand, considering that the magnetic resonance has not been detected in the single layer Bi2201 [20], magnetic modes should be ruled out as a general mechanism within a controllable theory of strong correlations. Recently, focusing on the phonon-coupling mechanism we have introduced a simple but realistic model built on the conventional Eliashberg strong coupling theory that allows one to reproduce the appearance of the ubiquitous nodal kink for a wide set of ARPES data in several HTSC systems and at several doping levels [21]. Let us recall that the electronic properties of the HTSC are strongly dependent on the doping level and therefore a systematic investigation of the ARPES spectra is due in order to extract key features relevant to high-T_c superconductivity. Along this line, $La_{2-x}Sr_xCuO_4$ (LSCO) appears as a highly suitable system, as far as the hole concentration in the CuO_2 planes is well controlled through the Sr content x and this allows to range from the undoped insulator $x = 0$ to the heavily overdoped metal ($x \sim 0.35$) [22]. This has motivated the choice of the LSCO system in a number of works [4, 6, 23].

In this paper, based on the above mentioned model [21] we report on the evolution of the electron band energy dispersion. We systematically cover the entire doping range for the LSCO system, determining the critical temperatures, the ratio gap, and other related parameters as a function of electron–phonon-coupling parameter "λ".

The paper is organized as follows. In Sect. 2, we discuss some details on the electron quasiparticle properties, the boson spectral density, and the theoretical treatment to be used. In Sect. 3 we present a systematic study of the influence of the boson-coupling parameter λ on the electron quasiparticle dispersions properties measured by ARPES. We will be focused on the nodal direction in LSCO at low energies. Then, we analyze its influence on the critical temperature T_c, the ratio gap $2\Delta_0/k_BT_c$, and the zero temperature gap Δ_0. An empirical equation is incorporated for determining λ from the doping level which may be of interest to other works. Finally, Sect. 4 is devoted to discussing our results. The relevance of the electron–phonon-coupling mechanism for the interpretation of the electron dynamics in HTSC will be concluded. Comparison with recent published material will be emphasized.

2 ARPES and the Electron–Phonon Coupling

Ordinary metals can be understood within the conventional Fermi-liquid picture, where electron-like quasiparticles populate bands in energy-momentum space up to the cut-off at the Fermi energy. Lattice vibrations couple to electrons because displacements of atoms from their equilibrium positions alter the band dispersions, lowering or raising the total electron quasiparticle energy. This phonon-mediated interaction between electrons, or electron–phonon coupling, has been long identified as the pairing mechanism responsible for superconductivity. In HTSC, on the contrary, it has been suggested that other collective excitation modes mediate the pairing since the superconducting transition temperature T_c is much higher than those for conventional superconductors. However, the recent observation of similar renormalization effects in the quasiparticle energy dispersion of HTSC has raised the hope that the mechanism of high-T_c superconductivity may finally be resolved [4–6, 19, 23].

The large impact of the ARPES technique on the many body theories stems from the fact that ARPES measurements provide a means of evaluating the quasiparticle self-energy $\Sigma(\mathbf{k}, \omega)$. In fact, the electronic structure of the material under study can be inferred from measuring the intensity of the photoemitted electrons as a function of their kinetic energy and their emission angle when the so-called sudden approximation is considered [21, 24, 25]. For more details on the photoemission techniques, the reader is referred to Refs. [1, 5]. Here, we are focused on the (0,0)–(π,π) direction in the Brillouin zone, known as nodal direction in order to avoid the anisotropic character of the superconducting gap beyond the s channel. In fact, it is well established that in the nodal direction the d-wave superconducting gap is zero in all HTSC [4, 6, 10, 13, 15, 26]. On the contrary, we recall that the antinodal direction denotes the $(0, \pi)$ region in the Brillouin zone, where the d-wave superconducting gap has a maximum [15]. Then, as related to its ability for measuring Σ and avoiding the complications

of the anisotropic superconducting gap, the ARPES experiments provide a unique opportunity to further explore the influence of the electron–phonon interaction on any relevant energy scale present that will manifest itself in the quasiparticle dynamics. In fact, in ARPES, the dressed electron quasiparticle dispersion relation (E_k) can be related to the bare band dispersion $\varepsilon_{\mathbf{k}}$ through the real part of the self-energy by $E_{\mathbf{k}} = \varepsilon_{\mathbf{k}} + \mathrm{Re}\Sigma(E_k)$ [21]. In global terms, this quantity characterizes the charge carriers as quasiparticles that are formed when the electrons are *dressed* with excitations. On the other hand, within the perturbative scheme of the Migdal–Eliashberg theory for dealing with the strong electron–phonon-coupling effects [27], the electron–phonon interaction self-energy may be obtained from the real part of the expression [28]

$$\Sigma\left(\omega + i0^{+}\right) = \int_0^{\infty} d\nu\, \alpha^2 F(\nu) \left\{ -2\pi i \left[N(\nu) + \frac{1}{2} \right] + \psi\left(\frac{1}{2} + i\frac{\nu - \omega}{2\pi T} \right) - \psi\left(\frac{1}{2} - i\frac{\nu + \omega}{2\pi T} \right) \right\}, \tag{1}$$

valid for the whole range of temperatures T, frequencies ν, and energies ω. Here, $\psi(z)$ are the so-called digamma functions with complex argument and $\alpha^2 F(\nu)$ defines the important electron–phonon spectral density which measures the effectiveness of the phonons of frequency ν in the scattering of electrons from any state to any other state on the Fermi surface. The hypotheses supporting the approximations behind this formula will not be discussed in detail here. In brief, one is basically assuming that the relevant electronic states for the process are close to the Fermi surface and they are well described by the lowest order Feynman graph for the electron–phonon interaction, as it has been more extensively discussed in our previous works [21, 27].

As a manifestation of electron–phonon-coupling interaction one introduces a mass renormalization in terms of the electronic dispersion at the energy scale associated with the phonons, i.e.: $E_{\mathbf{k}} \sim \varepsilon_{\mathbf{k}}/(1 + \lambda^*)$. On the other hand, the strength of the interaction is also related to the so-called boson-coupling parameter λ, which determines the superconducting transition temperature T_c. λ is commonly defined from the electron–phonon spectral density by $\lambda \equiv 2\int_0^{\infty} d\nu\, \alpha^2 F(\nu)/\nu$. Here, we want to emphasize that this quantity is not to be straightforwardly identified with the mass-enhancement parameter λ^* and a necessary distinction between them is essential for the overall description of the available ARPES data.

To avoid the intrinsic complexity in evaluating the matrix elements of the electron–phonon interaction that determine the spectral density $\alpha^2 F(\nu)$ from first principles, we focused on auxiliary experimental data. Here, we will refer

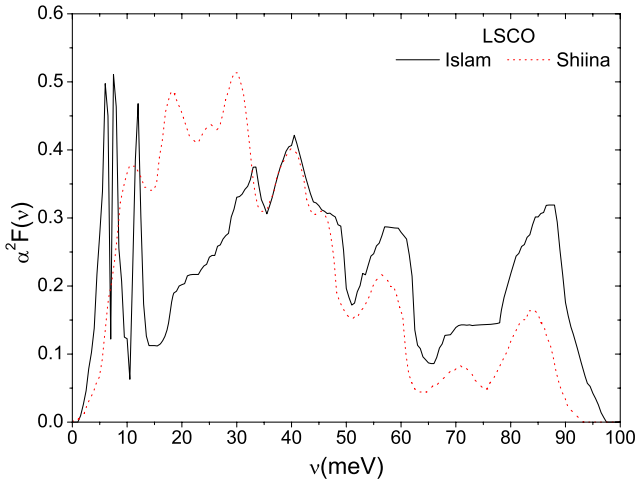

Fig. 1 (Color online) Electron–phonon spectral density $\alpha^2 F(\nu)$ of LSCO. *The black solid line* corresponds to the method of Ref. [30] and *the red line* (*dashed*) to the method of Ref. [29]

to an isotropic quasiparticle spectral density which can in turn be interpreted as the product between the phonon density of states $F(\nu)$ to be calculated from INS experiments at the phonon frequency ν, and the frequency-dependent electron–phonon-coupling term $\alpha^2(\nu)$. In this sense, we suggest the use of the spectral functions $\alpha^2 F(\nu)$ determined by Shiina and Nakamura [29] or independently by Islam and Islam [30], both based on the INS experimental data by Renker et al. [31] (see Fig. 1). Very similar results are found under the use of any of these densities. In order to avoid major complications over the determination of the electron–phonon spectral density we have chosen the model of Ref. [30] for two reasons: first, proper account has been taken of the irregular shape of the spectral function, and second, the sophisticated numerical solution of the Eliashberg equations can be avoided. On the other hand, we should comment that other choices of the spectral density where the interaction mechanism has a magnetic origin are possible but have been left aside because it does not seem to have a relevant character on the electron energy dispersion properties in LSCO. This issue will be reconsidered in our final discussion.

We have found that the experimental slopes of $\mathrm{Re}\{\Sigma(\mathbf{k}, \omega)\}$ at the low-energy kink give the electron–phonon-coupling parameter λ to the first perturbation order [21]. Then, the phonon interpretation receives strong support from a direct comparison between photoemission measurements and INS data on LSCO (Fig. 2). As the energy distribution and momentum distribution curves (EDC/MDC) are two most popular ways in analyzing photoemission data, the dichotomy between the MDC- and EDC-derived bands from the same data raises critical questions about its origin and which one represents intrinsic band structure. However, recalling the larger bandwidth along the

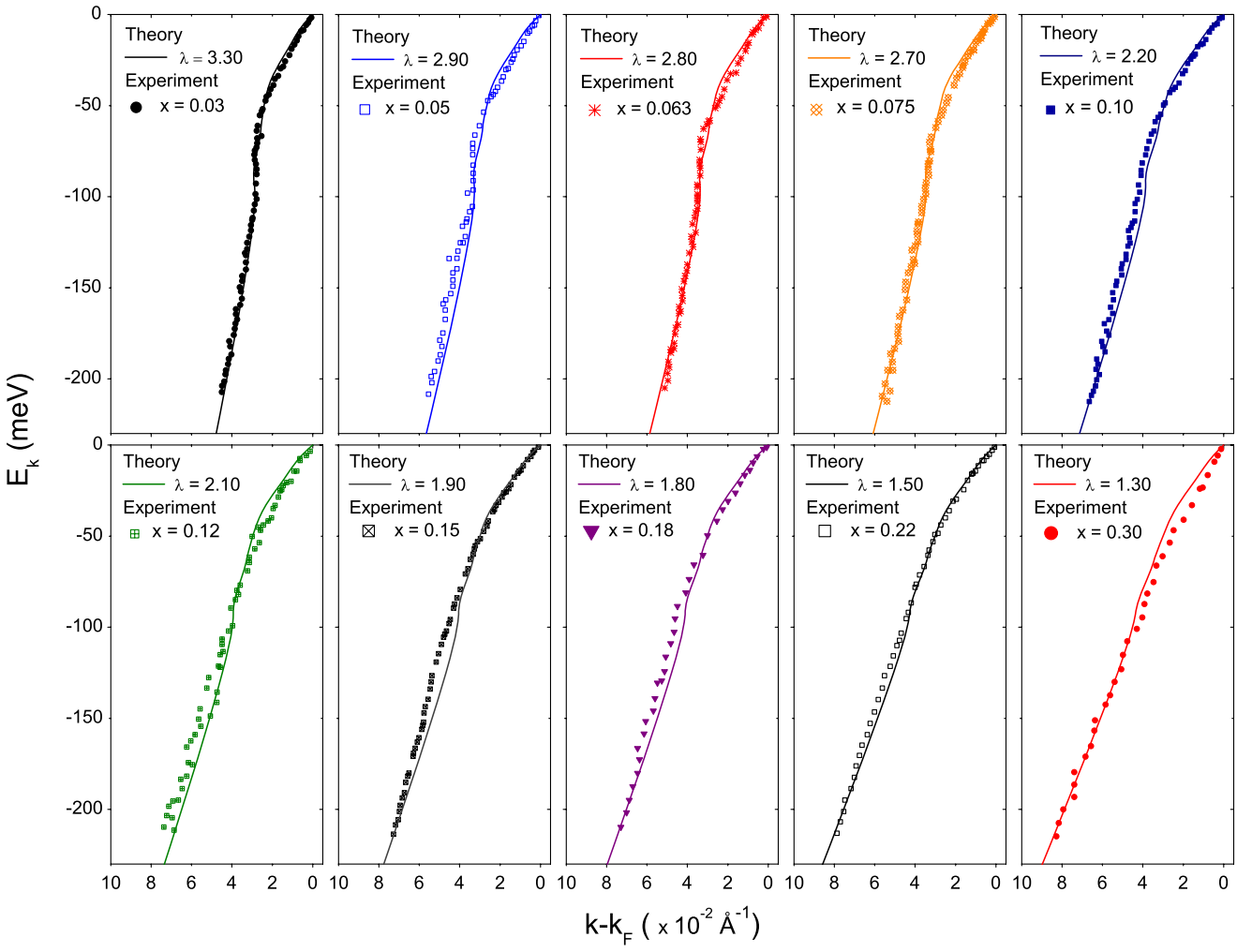

Fig. 2 The renormalized electron quasiparticle energy dispersion E_k as a function of the momentum $k - k_F$ for several samples of $La_{2-x}Sr_xCuO_4$ measured along the (0,0)–(π,π) nodal direction at a temperature of 20 K. The doping level x ranges between 0.03 (*top left*) up to 0.30 (*bottom right*). The experimental data (*symbols*) are taken from Ref. [4] and the theoretical curves (*solid lines*) have been obtained from the model introduced in Ref. [21]

nodal direction, the MDC method can be reliably used to extract high quality data of dispersion in searching for fine structure. It has also been shown theoretically that this approach is reasonable in spite of the momentum-dependent coupling if we are only interested in identifying the mode energies [32]. In a typical Fermi-liquid picture, the MDC- and EDC-derived dispersions are identical. Moreover, in an electron–boson-coupling system, unless very close to the kink region, the lower and higher energy parts of the MDC- and EDC-derived dispersions are still consistent [8]. The good agreement between our theoretical data and the experimental fact is consistent with this general picture.

3 On the Influence of the Coupling Parameter

Assuming that the kink effect observed for different HTSCs, over the entire doping range, and at different temperatures, has a common origin, the coupling of quasiparticles with phonons seems to be the only possible scenario [21]. There are a number of experimental features in the ARPES measurements that can be used to further check on the nature of the low-energy excitation involved, such as the topology of the energy- and momentum-dispersion curves. The key issue is the existence of an energy scale. Our position in this paper has been to obtain the bare electron band energy $\varepsilon_{\mathbf{k}}$ through the systematic evaluation of the influence of the electron–phonon-coupling parameter on the electron dressed band energy E_k. We recall that ε_k is not directly available from the experiments. Instead, the electron momentum-dispersion curve $E_k(k - k_F)$ may be measured from the ARPES experiments. This fact, along with some ansatz for the ARPES "bare" dispersion allows to obtain λ as a unique constrained parameter that better fits the observed kink topology in a particular sample [9, 11]. Nevertheless, the indiscriminate

proposal of dispersion relations could considerably underestimate or overestimate the average renormalization because implicit approximations are used [33]. Thus, based on an interpolation scheme between the numerical behavior of the dressed energy band and the experimental data, we introduce the universal dispersion relation [21]

$$k - k_F = \frac{\varepsilon_k}{v_{F_<}}(1 - \delta\lambda), \tag{2}$$

with $v_{F_<}$ the Fermi velocity at low energies. Contrary to the behavior at high-energy values, this limit of the Fermi velocity is rather independent of the chemical structure and doping levels within an experimental error of 20% and it is obtained as the slope of the lower part of the momentum-dispersion curve [4]. Thus, δ is the only "*free*" parameter required for incorporating the specific renormalization for a given superconductor. The physical meaning of the δ parameter is straightforwardly determined by recalling that the mass-enhancement parameter [28] is defined by $\lambda_k^* \equiv -\partial_\omega \Sigma_1|_{\omega=0}$. Thus, after some algebra, one obtains $\delta = (\lambda^*/\lambda)/(1 + \lambda^*)$. To the lowest order, the dimensionless parameter δ is basically the ratio between the mass-enhancement and phonon-coupling parameters, i.e.: $\delta \approx \lambda^*/\lambda$. Outstandingly, it will be shown that this fact reassembles the differences obtained by tight-binding Hamiltonian models [29, 34] and the "density-functional" band theories [9, 16]. As it will be seen below, predictions from both types of models may be reconciled appealing to the differences between λ and λ^* (Table 1). Thus, from our view, the coupling coefficient calculated from the DFT self-energy must be basically identified to λ^*, instead of the electron–phonon coupling λ, involved in the standard Migdal formalism analysis of experiments [21]. Recall that, in principle, the DFT gives a correct ground state energy, but the bands do not necessarily fit the quasiparticle band structure used to describe the low-lying excitations [9].

In Fig. 3 we show the singular features involved within the bare electron band energy curves $[E_k(\varepsilon_k)]$ and the renormalized dressed electron band energies $[E_k(k - k_F)]$. One can observe a structure in the renormalized quasiparticle energy E_k ranging up to roughly 80 meV. In fact, the bands rapidly approach E_F from high-binding energy and suddenly bend at 40–80 meV, showing the kink topology described in the ARPES experiments. Here, we also recall some anomaly within the dispersion of the lines around $\lambda = 1.75$ revealing the existence of a maximal peak in the MDC along the nodal direction.

For quantitative purposes, here, we have considered $v_{F_<} = 2$ eV·Å as related to the experimental results of Refs. [4–6, 10]. On the other hand, the best fit of the whole set of experimental data has been obtained for $\delta = 0.185$ (Fig. 2), and the derived λ^* values to first perturbation order are shown in Table 1. The evolution of the λ parameter as a function of the doping level is shown in

Table 1 Electron–phonon-coupling parameter λ and the corresponding mass-enhancement parameter λ^* obtained from the analysis of ARPES data at several doping levels x of LSCO (see Fig. 2). λ^* has been obtained to the lowest order approximation $\lambda^* \approx \delta\lambda$ (in this case $\delta = 0.185$), and the critical temperatures from the McMillan's formula [35]. Our results are presented in contrast with other models available in the literature

x	Ref.	λ	λ^*	$T_c(\lambda)$ [K]
0.03	This[a]	3.30	0.61	–
0.05		2.90	0.54	–
0.063		2.80	0.52	–
0.075		2.70	0.50	–
0.10		2.20	0.41	42.10
0.12		2.10	0.39	40.77
0.15		1.90	0.35	37.83
0.18		1.80	0.33	36.19
0.22		1.50	0.28	30.47
0.30		1.30	0.24	–
0.1–0.2	[34][b]	2–2.5	–	30–40
–	[29][b]	1.78	–	40.6
0.15	[16][c]	1–1.32	0.14–0.22	–
0.22	[16][c]	0.75–0.99	0.14–0.20	–

[a]We allow a margin of error in λ of $\sim \pm 0.3$ as related to the numerical interpolation procedure between theory and experiment

[b]The λ values reported in that reference were obtained so as to fit T_c at the indicated values

[c]In Ref. [16] the electronic structure of LSCO has been calculated employing a generalized gradient approximation to density functional theory and used to determine λ

Fig. 4. Taking advantage of the widespread availability of experimental data in LSCO system one can fit the data to the simple expression $\lambda = 2\tilde{\omega}\exp(-\frac{\tilde{\omega}}{\delta}) + 1$, within a precision factor around of 95%. $\tilde{\omega}$ is the ratio between the phonon characteristic energies introduced by McMillan [35], $\omega_1 = (2/\lambda)\int_0^\infty \alpha^2 F(\nu)\,d\nu \equiv (2/\lambda)S$, and Allen and Dynes [36], $\omega_{\log} \equiv \exp\{(2/\lambda)\int_0^\infty \ln(\nu)[\alpha^2 F(\nu)/\nu]\,d\nu\}$, i.e., $\tilde{\omega}$=$\omega_1/\omega_{\log}$. We get $\omega_{\log}^{\mathrm{LSCO}} \simeq 16.1455$ meV and $\omega_1^{\mathrm{LSCO}} \simeq 25.2627$ meV. We want to clarify that, although this equation can be considered as just a useful relation between the physical and chemical properties of LSCO system, the shaping of other HTSC by similar expressions cannot be guaranteed. Regarding the critical temperatures, it must be emphasized that for the LSCO system, the λ-values obtained from our model [21] allow to explain the observed superconducting temperatures T_c [37–39]. This can be done either by using the McMillan formula [35] or in a more general way, by solving the Eliashberg equations [29]. Nevertheless, we want to give clarity on how these facts have to be interpreted with the purpose of recalling that several discrepancies could be emerge depending on the formula used for obtaining T_c.

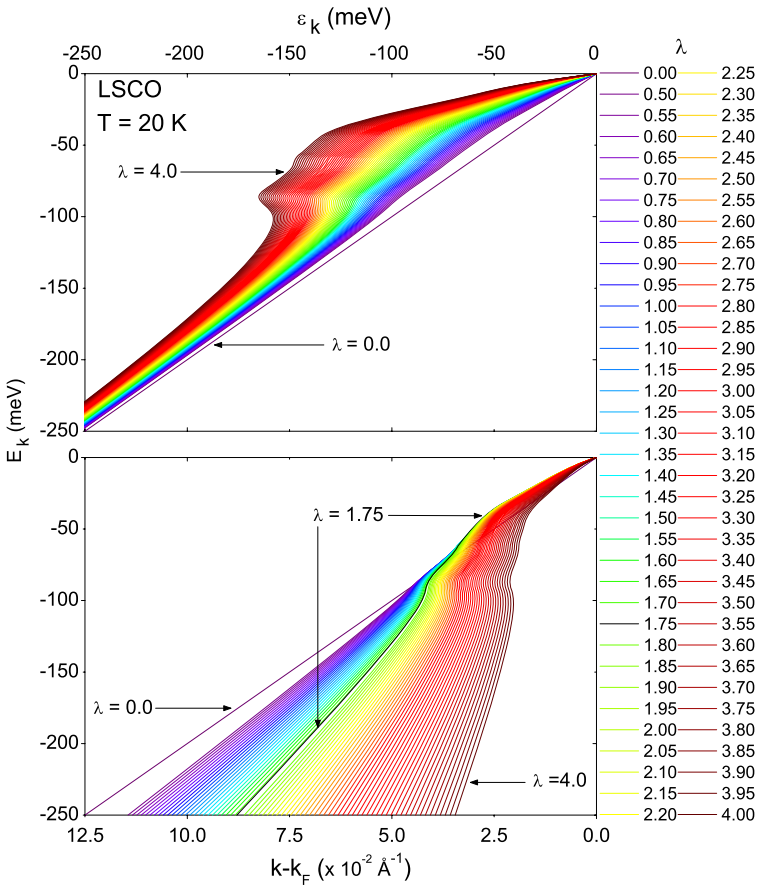

Fig. 3 (Color online) The renormalized energy E_k as a function of the bare band energy (*top*) and momentum $k - k_F$ (*bottom*) for the nodal dispersion in LSCO. *The upper panel curves* have been obtained by using Eq. 1 and the EPI spectral density $\alpha^2 F(\omega)$ that comes from the method of the Ref. [30] (Fig. 1). *The lower panel* has been produced starting from our renormalization formula (Eq. 2) that re-adjusts the momentum-dispersion curves. *The curves* are labeled according to the e-ph coupling parameter "λ" between the bare dispersion $\lambda = 0.0$ (*straight line*) and about $\lambda = 4.0$. All the results are at a common temperature $T = 20$ K

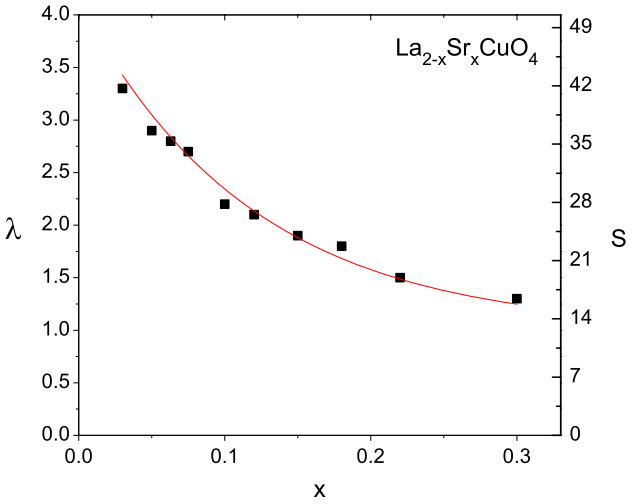

Fig. 4 (Color online) Evolution of the e-ph coupling parameter λ as a function of the dopant content in $La_{2-x}Sr_xCu_4$ samples. The λ-values have been obtained from our best adjustment with the nodal kink dispersion (*black squares*) showed in the Fig. 2. Correspondingly, the evolution of the area S as a function of the dopant content is also shown (*right scale*)

Let us go into some more detail. From the above discussion, it can be concluded that, the critical temperature T_c should be not considered as a fit parameter for adjusting the theory, i.e.: one should not predict λ from the approximate T_c formulas and then use it for calculating the electron self-energy. In fact, this attractive idea has led to unfortunate underestimates of the phonon contribution to the photoemission kink in HTSC [16, 42]. Related to this, we show the comparison of the results obtained from several popular expressions. Thus, in Fig. 5 we show the dependencies for the critical temperatures T_c, the so-called ratio gap $2\Delta_0/k_BT_c$ and the zero temperature gap Δ_0, based on three different formulations: (i) the celebrated McMillan's equation [35], $T_c = (\omega_1/1.2)\exp[-1.04(1+\lambda)/(\lambda-\mu^*(1+0.62\lambda))]$, (ii) the Allen and Dynes formula [36] which is obtained by replacing ω_1 by $\omega_{\log}$, and (iii) the less conventional Kresin's formula [40, 41] $T_c = 0.25\varpi\exp(2/\lambda_{\text{eff}} - 1)^{-1/2}$ where $\varpi = [(2/\lambda)\int_0^\infty \nu\alpha^2F(\nu)\,d\nu]^{1/2}$ and, $\lambda_{\text{eff}} = (\lambda - \mu^*)[1 + 2\mu^* + (3/2)\lambda\mu^*\exp(-0.28\lambda)]$. The Coulomb's pseudopotential was given a typical value [28], $\mu^* = 0.13$. The ratio gap has been calculated by using the expression $2\Delta_0/k_BT_c = 3.53[1 + 12.5(T_c/\omega_{\log})^2\ln(\omega_{\log}/2T_c)]$. Then, from Fig. 5, is concluded that the use of an arbitrary approximative formula to determine the coupling parameter λ from T_c could lead to strong under or overestimates of the strength of the boson-coupling mode mediated pairing interaction in a HTSC. To our knowledge, the most suitable way for determining the influence of an interaction mecha-

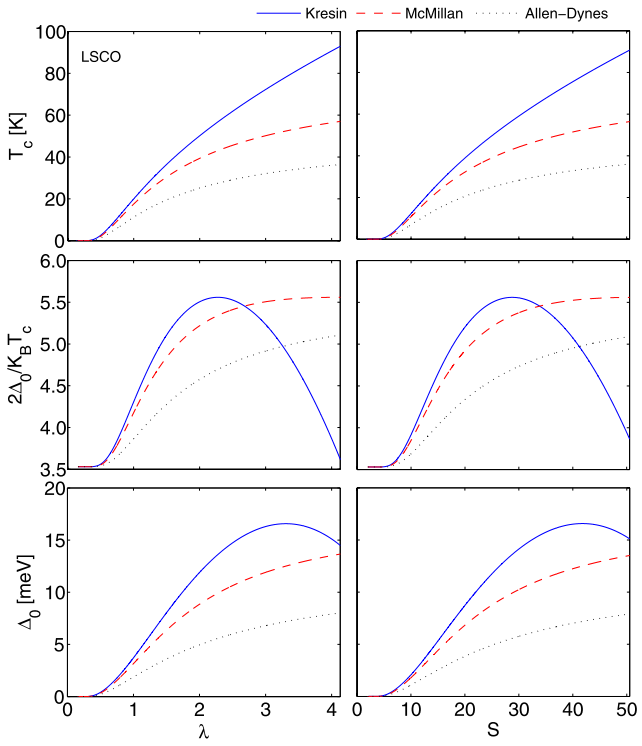

Fig. 5 (Color online) Plot of the critical temperatures T_c (*top*) for the LSCO from the Kresin's formula [40, 41] (*blue solid line*), McMillan's formula [35] (*red dashed line*), and the Allen-Dynes formula [36] (*black dotted line*). The different curves have been represented as functions of the electron–phonon-coupling parameter λ (*left*) and the area S (*right*). Corresponding to it the gap ratio $2\Delta_0/k_B T_c$ (*middle*) and the gap Δ_0 (*bottom*) are shown

nism in the pair formation for HTSC could be (i) to evaluate the strength of the boson-coupling mode from the electron renormalization effects and then (ii) solve the Eliashberg equations for the superconducting T_c. A semiempirical approach has been introduced in this paper by using the celebrated equations for $T_c(\lambda)$ referred above. From such analysis, we conclude that the consideration of the electron–phonon interaction in LSCO strongly suggests that the high T_c values can be caused by conventional electron–phonon coupling, in agreement with the conclusion of Weber [34].

More work is necessary for establishing the relative importance of the boson contributions (phonons, spin fluctuations, etc.) on the electron band renormalization effects and their influence on the high superconducting temperatures for other copper oxides [7–9, 11–14, 19, 21, 23, 43, 44].

As a further detail, very recent efforts have been focused on the high-energy part of the ARPES data (0.2–1.5 eV) revealing additional changes in the electron energy dispersion "*waterfalls*" at ∼0.4 eV [7, 8, 12, 23, 43]. The presence of a kink at these high energies immediately raises the question: what type of excitation spectrum is required to produce such renormalization effect? One possibility is that correlation effects at high orders strongly renormalize the electron–phonon coupling [21]. Nevertheless, these high-energy features remain under intense debate [7, 8, 12, 23, 43, 45, 46] because it is still unclear whether they represent intrinsic band structure or not [8].

Related to the limitations introduced by the use of the electron–phonon-coupling parameter, one should mention that, long before the advent of the high temperature superconductivity, Ashcroft and Wilkins [47] showed that in some simple metals the single parameter λ is insufficient to determine a number of thermodynamic properties such as the specific heat. Therefore, it is not surprising that similar anomalies may appear in the HTSC. The clarification of these issues is important in establishing a basic theoretical framework to describe strongly correlated electron systems like HTSC, in probing electron dynamics by extracting electron self-energy, and in unraveling possible new physics.

4 Conclusions

In summary, although the role of electron–phonon coupling for high-T_c superconductivity is unclear yet, our results suggest that at least in LSCO compounds the electron–phonon interaction is the most relevant mechanism involved in the pairs formation that leads at the superconductivity. Our conclusion is supported by the experimental evidence of a mass renormalization of the electronic dispersion curves measured along the nodal direction in ARPES and the reported T_c values that are in good agreement with our theoretical predictions. A excellent comparison between the theory and the available collection of experiments is achieved. Moreover, we have shown that the maximal value expected for the critical temperature ($T_c \sim 40$ K) is predicted within our model, in which the difficulties imposed by the anisotropic character of the gap function can be avoided. Thus, it is beyond any doubt that the phonon-coupling mode strongly influences the electron dynamics in the high-T_c superconductors, and it is an important mechanism linked with the Fermi surface topology. Then, the electron–phonon interaction (strong or weak) must be included in any realistic microscopic theory of superconductivity.

On the other hand, with the aim to predict the high-T_c observed in other materials, we want to mention that the enhancement of the electron correlations involved in the coupling to bond-stretching phonons as well as other possible coupling modes are not discarded. Moreover, although in the LSCO system the influence of the magnetic mode seems not relevant, it is not possible ignore its importance over the electron properties of other HTSC families [21]. In fact, the recent observation by G. Yu et al. [48] of a connection between the magnetic excitations and the superconductor gap for a wide range of materials seems indicate that it could also play an important role on the superconducting pair formation.

Acknowledgement This work was supported by Spanish CICyT projects MAT2008-05983-C03-01 and MTM2006-10531. H.S. Ruiz acknowledges a grant from Spanish CSIC (JAE program).

References

1. Hüfner, S. (ed.): Very High Resolution Photoelectron Spectroscopy. Springer, Berlin (2007)
2. Kúlic, M.L.: Phys. Rep. **338**, 1 (2000)
3. Smith, N.V.: Phys. Rev. B **64**, 155106 (2001)
4. Zhou, X.J., Yoshida, T., Lanzara, A., Bogdanov, P.V., Kellar, S.A., Shen, K.M., Wang, W.L., Ronning, F., Sasagawa, T., Kakeshita, T., Noda, T., Eisaki, H., Uchida, S., Lin, C.T., Zhou, F., Xiong, J.W., Ti, W.X., Zhao, Z.X., Fujimori, A., Hussain, Z., Shen, Z.-X.: Nature **423**, 398 (2003)
5. Zhou, X.J., Cuk, T., Devereaux, T., Nagaosa, N., Shen, Z.-X.: Handbook of High-Temperature Superconductivity. Springer, New York (2007). Chap. 3, p. 87
6. Lanzara, A., Bogdanov, P.V., Zhou, X.J., Kellar, S.A., Feng, D.L., Lu, E.D., Yoshida, T., Eisaki, H., Fujimori, A., Kishio, K., Shimoyama, J.-I., Noda, T., Uchida, S., Hussain, Z., Shen, Z.-X.: Nature **412**, 510 (2001)
7. Graf, J., d'Astuto, M., Jozwiak, C., Garcia, D.R., Saini, N.L., Krisch, M., Ikeuchi, K., Baron, A.Q.R., Eisaki, H., Lanzara, A.: Phys. Rev. Lett **100**, 227002 (2008)
8. Zhang, W., Liu, G., Meng, J., Zhao, L., Liu, H., Dong, X., Lu, W., Wen, J.S., Xu, Z.J., Gu, G.D., Sasagawa, T., Wang, G., Zhu, Y., Zhang, H., Zhou, Y., Wang, X., Zhao, Z., Chen, C., Xu, Z., Zhou, X.J.: Phys. Rev. Lett. **101**, 017002 (2008)
9. Reznik, D., Sangiovanni, G., Gunnarsson, O., Devereaux, T.P.: Nature **455**, E6 (2008)
10. Zhou, X.J., Shi, J., Yoshida, T., Cuk, T., Yang, W.L., Brouet, V., Nakamura, J., Mannella, N., Komiya, S., Ando, Y., Zhou, F., Ti, W.X., Xiong, J.W., Zhao, Z.X., Sasagawa, T., Kakeshita, T., Eisaki, H., Uchida, S., Fujimori, A., Zhang, Z., Plummer, E.W., Laughlin, R.B., Hussain, Z., Shen, Z.-X.: Phys. Rev. Lett. **95**, 117001 (2005)
11. Dahm, T., Hinkov, V., Borisenko, S.V., Kordyuk, A.A., Zabolotnyy, V.B., Fink, J., Büchner, B., Scalapino, D.J., Hanke, W., Keimer, B.: Nature Phys. **5**, 217 (2009)
12. Graf, J., Gweon, G.-H., McElroy, K., Zhou, S.Y., Jozwiak, C., Rotenberg, E., Bill, A., Sasagawa, T., Eisaki, H., Uchida, S., Takagi, H., Lee, D.-H., Lanzara, A.: Phys. Rev. Lett **98**, 067004 (2007)
13. Kordyuk, A.A., Borisenko, S.V., Zabolotnyy, V.B., Geck, J., Knupfer, M., Fink, J., Büchner, B., Lin, C.T., Keimer, B., Berger, H., Pan, A.V., Komiya, S., Ando, Y.: Phys. Rev. Lett. **97**, 017002 (2006)
14. Terashima, K., Matsui, H., Hashimoto, D., Sato, T., Takahashi, T., Ding, H., Yamamoto, T., Kadowaki, K.,: Nature Phys. **2**, 27 (2006)
15. Xiao, Y.X., Sato, T., Terashima, K., Matsui, H., Takahashi, T., Kofu, M., Hirota, K.: Physica C **463–465**, 44 (2007)
16. Giustino, F., Cohen, M.L., Louie, S.G.: Nature **452**, 975 (2008)
17. Wilson, S.D., Dai, P., Li, S., Chi, S., Kang, H.J., Lynn, J.W.: Nature **442**, 59 (2006)
18. Zhao, J., Dai, P., Li, S., Freeman, P.G., Onose, Y., Tokura, Y.: Phys. Rev. Lett. **99**, 017001 (2007)
19. Park, S.R., Song, D.J., Leem, C.S., Kim, Chul, Kim, C., Kim, B.J., Eisaki, H.: Phys. Rev. Lett. **101**, 117006 (2008)
20. Sato, T., Matsui, H., Takahashi, T., Ding, H., Yang, H.-B., Wang, S.-C., Fujii, T., Watanabe, T., Matsuda, A., Terashima, T., Kadowaki, K.: Phys. Rev. Lett. **91**, 157003 (2003)
21. Ruiz, H.S., Badía Majós, A.: Phys. Rev. B **79**, 054528 (2009)
22. Ino, A., Kim, C., Nakamura, M., Yoshida, T., Mizokawa, T., Fujimori, A., Shen, Z.-X., Kakeshita, T., Eisaki, H., Uchida, S.: Phys. Rev. B **65**, 094504 (2002)
23. Chang, J., Shi, M., Pailhés, S., Månansson, M., Claesson, T., Tjernberg, O., Bendounan, A., Sassa, Y., Patthey, L., Momono, N., Oda, M., Ido, M., Guerrero, S., Mudry, C., Mesot, J.: Phys. Rev. B **78**, 205103 (2008)
24. Randeria, M., Ding, H., Campuzano, J.C., Bellman, A., Jennings, G., Yokoya, T., Takahashi, T., Katayama-Yoshida, H., Mochiku, T., Kadowaki, K.: Phys. Rev. Lett. **74**, 4951 (1995)
25. Koralek, J.D., Douglas, J.F., Plumb, N.C., Sun, Z., Fedorov, A.V., Murnane, M.M., Kapteyn, H.C., Cundiff, S.T., Aiura, Y., Oka, K., Eisaki, H., Dessau, D.S.: Phys. Rev. Lett. **96**, 017005 (2006)
26. Borisenko, S.V., Kordyuk, A.A., Zabolotnyy, V., Geck, J., Inosov, D., Koitzsch, A., Fink, J., Knupfer, M., Büchner, B., Hinkov, V., Lin, C.T., Keimer, B., Wolf, T., Chiuzbăian, S.G., Patthey, L., Follath, R.: Phys. Rev. Lett **96**, 117004 (2006)
27. Ruiz, H.S., Giraldo, J.J., Baquero, R.: J. Supercond. Nov. Magn. **21**, 21 (2008)
28. Allen, P.B., Mitrović, B.: In: H., Ehrenreich, F., Seitz, D., Turnbull (eds.) Solid State Phys., p. 1. Academic, New York (1982)
29. Shiina, Y., Nakamura, Y.O.: Sol. State Commun. **76**, 1189 (1990)
30. Islam, A.T.M.N., Islam, A.K.M.A.: J. Supercond. **13**, 559 (2000)
31. Renker, B., Apfelstedt, I., Küpfer, H., Politis, C., Rietschel, H., Schauer, W., Wühl, H., Gottwick, U., Kneissel, H., Rauchschwalbe, U., Spille, H., Steglich, F.: Z. Phys. B **67**, 15 (1987)
32. Devereaux, T.P., Cuk, T., Shen, Z.-X., Nagaosa, N.: Phys. Rev. Lett. **93**, 117004 (2004)
33. Schachinger, E., Tu, J.J., Carbotte, J.P.: Phys. Rev. B **67**, 214508 (2003)
34. Weber, W.: Phys. Rev. Lett. **58**, 1371 (1987)
35. McMillan, W.L.: Phys. Rev. **167**, 331 (1968)
36. Allen, P.B., Dynes, R.C.: Phys. Rev. B **12**, 905 (1975)
37. Bednorz, J.G., Müller, K.A.: Z. Phys. B **64**, 18 (1986)
38. Uchida, S., Takagi, H., Kishio, K., Kitazawa, K., Fueki, K., Tanaka, S.: Jpn. J. Appl. Phys. **26**, L443 (1987)
39. Dietrich, M.R., Fietz, W.H., Ecke, J., Obst, B., Politis, C.: Z. Phys. B **66**, 283 (1987)
40. Kresin, V.: Phys. Lett. A **122**, 434 (1987)
41. Wolf, S.A., Kresin, V.Z.: In: Mihailovic, D., et al. (eds.) Proc. of the International Workshop on Anharmonic Properties of High-T_c Cuprates, p. 232. World Scientific, Singapore (1995)
42. Heid, R., P Bohnen, K.-, Zeyher, R., Manske, D.: Phys. Rev. Lett. **100**, 137001 (2008)
43. Valla, T., Kidd, T.E., Yin, W.-G., Gu, G.D., Johnson, P.D., Pan, Z.-H., Fedorov, A.V.: Phys. Rev. Lett. **98**, 167003 (2007)
44. Reznik, D., Pintschovius, L., Ito, M., Likubo, S., Sato, M., Goka, H., Fujita, M., Yamada, K., Gu, G.D., Tranquada, J.M.: Nature **400**, 1170 (2006)
45. Zhu, L., Aji, V., Shekhter, A., Varma, C.M.: Phys. Rev. Lett. **100**, 057001 (2008)
46. Tan, F., Wang, Q.-H.: Phys. Rev. Lett. **100**, 117004 (2008)
47. Ashcroft, N.W., Wilkins, J.W.: Phys. Lett. **14**, 285 (1965)
48. Yu, G., Li, Y., Motoyama, E.M., Greven, M.: arXiv:0903.2291v1 (2009)